

Experimental Investigation of Friction and Slip at the Traction Interface of Rope and Sheave

Xiaolong Ma, Xi Shi

School of Mechanical Engineering, Shanghai Jiao Tong University,
800 Dong-chuan Road, Shanghai 200240, P. R. China

Keywords: Rope-sheave interaction, Slippage, Digital image measurement

Abstract. In this paper, an exclusive testing rig was built to experimentally investigate the friction and slip at elevator traction interface under different traction conditions. The effect of pre-tension of rope is also discussed which indicates that the full slip occurs earlier and is greater under smaller pre-tension force. The experimental results indicated that slipping occurs at both ends of contact arc first, and then expands to the middle region gradually until the full slip along the sheave occurs. In addition, the full slip occurs earlier under lower rope pre-tension.

1 INTRODUCTION

Early studies on friction between rope and sheave are very limited. The most famous formula was published by Eytelwein [1], who concluded with a fully exponential distribution of normal pressure and rope tension at full slip based on Euler's solution [2]. However, the deduction of the Euler-Eytelwein formula only considered the axial forces in the rope, and Heller [3] extended Euler's work to account for radial shear stresses in the rope by introducing a new parameter of diameter ratio D/d . Usabiaga etc. [4] provided a new model based on a similar assumption as that of Euler-Eytelwein formula, in which the behavior of the wire rope was simplified as a series of elastic springs and body elements. However, Lugićs etc. [5] stated that modeling the rope as a linear spring, although very simple and efficient, is not accurate if the rope deformation along the segment in contact with the sheave is not considered.

In term of experiments, Nabijou and Hobbs [6-8] did a series of research on wire ropes bent over sheaves. The relative movements between wires within a wire rope were first investigated to form a valuable input in predicting wire rope fatigue and then the curvature of wires in single and double helices during bending was calculated to examine the bending strains of wires in a frictionless rope. In addition, Wiek [9] measured the distribution of the local contact pressure in a particular U groove pulley under full stick condition. Inspired by his experiment, Usabiaga etc. [10] developed a similar experimental method to investigate how the imbalance ratio, defined as ratio of rope tensions (T_1/T_2) at ends of the rope, influences the distribution of normal contact pressure by embedding a tri-axial piezo-electronic load cell inside the sheave and measuring the resultant normal and tangential forces.

Feyrer [11] experimentally studied the influence of rope bending stiffness on the contact angle, and identified high local stresses at the ends of contact arc. Such phenomenon was also observed by Ridge etc. [12], in which the cyclic bending strain in the wires of a six-strand right-handed Lang's lay steel wire rope was measured as it was running on and off a pulley. The result showed that all cyclic bending strain signals demonstrate a similar waveform with two peaks: one as the rope moves on the pulley and the other as it moves off. Chen etc. [13] developed a wireless detection system for dynamic rope skid in a friction lifting system. With two child nodes installed on the friction drive wheel and the guide pulley respectively, this detection system was able to send speed signals of friction drive wheel and guide pulley to the host node, which could then calculate the speed difference to monitor the rope skid phenomenon. The disadvantage of their measurement is apparent in that the results present only the overall slippage of the rope, and the information about the slippage distribution is missed. In Oplatka and Roth's work [14], this problem was overcome by fixing a camera and a

floodlight on the sheave while rotating. The images of specific points on the rope were captured by the camera, which enabled the calculation of the relative speed between the sheave and the rope.

Although lots of experimental work has been done in investigation of traction drive system, the measurement of slippage evolution and distribution is scarce in the literature. In this work, a new experimental method for detecting dynamic slippage evolution by utilizing image processing technology was developed.

2 THE EULER-EYTELWEIN FORMULA

The traction is usually calculated with the Euler-Eytelwein formula. Figure 1a presents the traction interface between rope–sheave. Consider a differential rope element as shown in Fig.1b and assume the rope does not reach the state of gross slip and ignore the inertia forces, the equivalence of normal forces gives:

$$T(\alpha)\sin\frac{d\alpha}{2}+[T(\alpha)+dT]\sin\frac{d\alpha}{2}=p(\alpha)\frac{D}{2}d\alpha \quad (1)$$

The equivalence of tangential forces together with Coulomb friction law gives:

$$(T+dT)\cos\frac{d\alpha}{2}-T\cos\frac{d\alpha}{2}=fp(\alpha)\frac{D}{2}d\alpha \quad (2)$$

Since the differential angular extent $d\alpha$ is very small, Eq. (1) and Eq. (2) can be simplified as:

$$p(\alpha)=\frac{2}{D}T(\alpha) \quad (3)$$

$$dT=fp(\alpha)\frac{D}{2}d\alpha \quad (4)$$

Combining Eq.(3) and Eq.(4), the Euler-Eytelwein formula is obtained as below:

$$T_1/T_2=e^{f\theta} \quad (5)$$

where T_1 (high tension) and T_2 (low tension) are the rope tensions at both ends as shown in Fig.1a, θ the rope wrap angle, f the equivalent COF, $p(\alpha)$ the distribution of the normal line contact pressure and D is the sheave diameter.

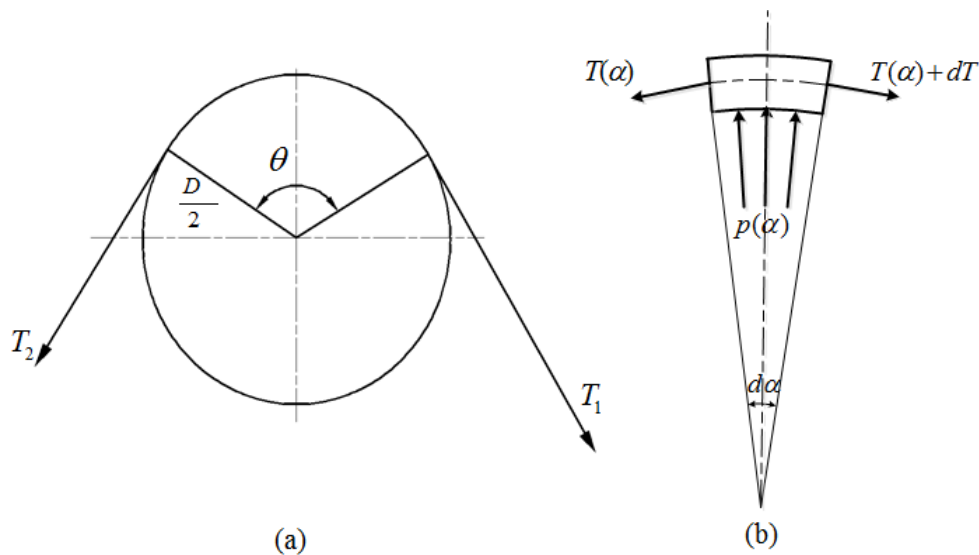


Figure 1 Geometry and notation for contact forces at rope–sheave interaction

The traction friction between the rope and the traction sheave results in a rope tension difference between two ends thus provides the traction capability. For a given traction system, the traction capability depends on the maximum friction at the rope-traction sheave interface which is governed by the Euler-Eytelwein formula. In principle, three traction conditions can be determined by comparing the rope tension ratio to the maximum value predicted by Euler-Eytelwein formula: (1) if $T_1 / T_2 < e^{f\theta}$, the traction of this system is large enough; (2) if $T_1 / T_2 = e^{f\theta}$, then the rope sliding is pending and any disturbance may trigger the slip, thus it is not safe; and (3) if $T_1 / T_2 > e^{f\theta}$, the rope slips on the traction sheave and the traction drive system is not safe as well.

Note that as the simplest theoretical model concerning traction drives, the Euler-Eytelwein formula neglects some factors, including the diameter ratio of sheave and rope, rope weight, the angular velocity of sheave and so on.

3 EXPERIMENTS

3.1 Test rig

The schematic of the test rig is shown in Fig.1. In this test rig, two identical motors (model KONE MX18) are used, one of which is used to drive the traction sheave, and the other is used to provide a constant torque load to simulate the moment due to the elevator system gravity. Two fly wheels are designed to account for the system inertia and a 5:1 gear box is adopted to increase the rotation speed of the fly wheel thus reduce the required fly wheel size.

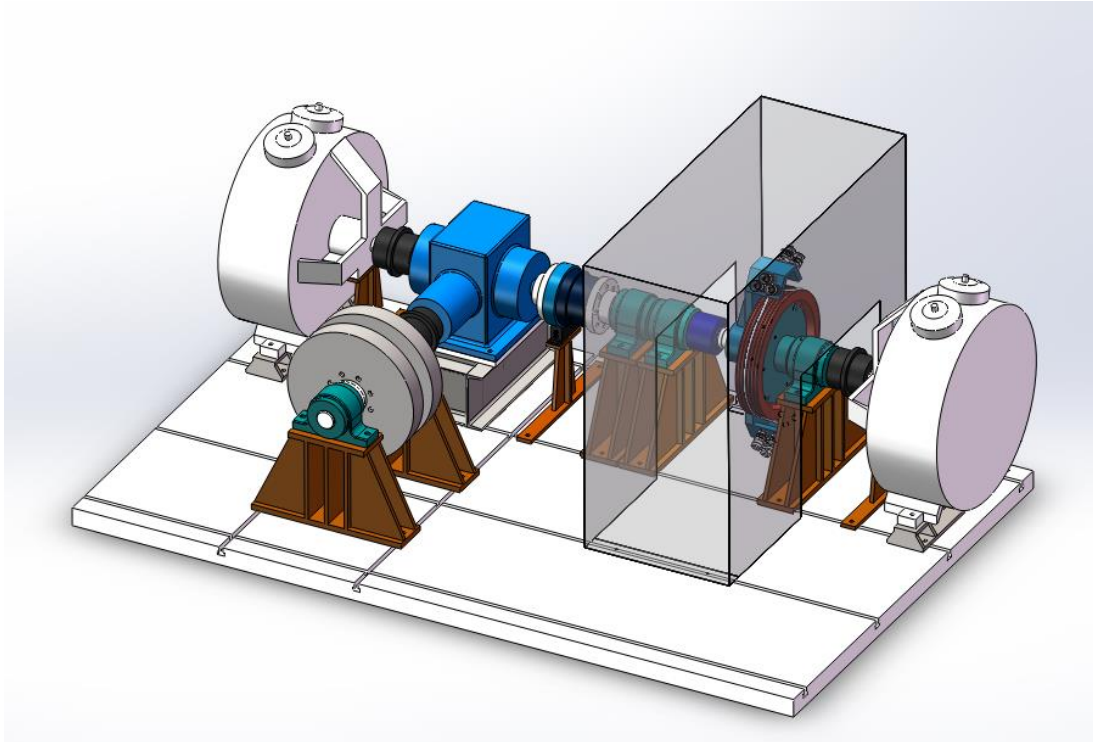


Figure 1 Schematic of the whole test rig

The traction interface consists of the traction sheave and six piece of wire ropes which are wrapped on the traction sheave symmetrically as shown in Fig.2. The ropes ends are fixed on a specially designed fork frame and the rope tension is adjustable with disk springs and screw assemble before the tests. The instantaneous tension force for each rope end during the test is measured with a load cell sandwiched between the disk springs and the nut.

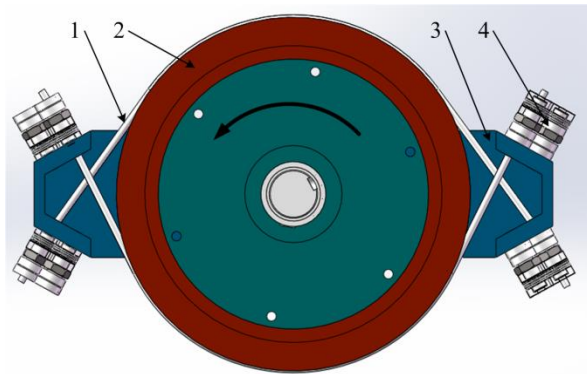


Figure 2 Assembly of traction system: 1-rope, 2-traction sheave, 3-fork frame, 4-rope fixture

3.2 Measurement of rope slippage

Figure 3 depicts the rope slippage measurement system, which consists of a high speed industrial camera (JAI SP-5000C-PMCL), LED light source, the marked object and a computer for image processing.



Figure 3 Structure of slippage measuring equipment

A series of mark sets are purposely made along the traction interface and each set consists of three mark points: one on the wire rope and two on the lateral side of the traction sheave near the edge as shown in Fig.4a. During the traction, the relative positions of those mark sets were recorded with a high speed industrial camera and the raw images are processed first with five detailed processes: image reading, threshold calculation and binarization, dilation, erosion and opening operation. Besides, the experiment for camera calibration was performed by using a circle with diameter 10 mm as calibration pattern. And the results show that the measurement error of displacement is roughly in the range of 0.2mm~0.22mm.

Geometrical relationship of slippage can be calculated after image processing. As shown in Fig.4b, two sequential pictures were taken by the camera and the mark set of former moment is represented as AB_1C while the mark set of latter moment is represented as AB_2C . The relative slippage between the two cases is very small because of very short exposure time, the length of straight line B_1B_2 is assumed to be equal to the arc length of B_1B_2 , thus the approximated slippage of the rope B_1B_2 can be derived as below:

$$\overline{B_1B_2} = \sqrt{\overline{AB_1}^2 + \overline{AB_2}^2 - 2\overline{AB_1} \cdot \overline{AB_2} \cdot \angle B_1AB_2} \quad (6)$$

There are two cases need to be considered in determining the value of $\angle B_1AB_2$.

Case1: if point A locates outside $\triangle CB_1B_2$:

$$\angle B_1AB_2 = |\angle CAB_1 - \angle CAB_2| \quad (7)$$

Case2: if point A locates inside $\triangle CB_1B_2$:

$$\angle B_1AB_2 = 2\pi - (\angle CAB_1 + \angle CAB_2) \quad (8)$$

Where

$$\angle CAB_1 = \arccos\left(\frac{\overline{AB_1}^2 + \overline{AC}^2 - \overline{B_1C}^2}{2\overline{AB_1} \cdot \overline{AC}}\right) \quad (9)$$

$$\angle CAB_2 = \arccos\left(\frac{\overline{AB_2}^2 + \overline{AC}^2 - \overline{B_2C}^2}{2\overline{AB_2} \cdot \overline{AC}}\right) \quad (10)$$

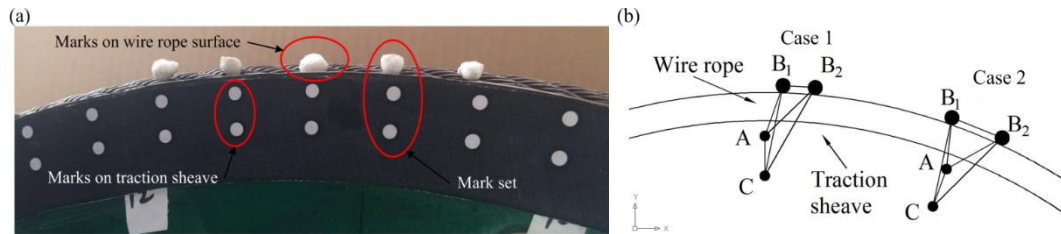


Figure 4 Calculation of slippage (a) mark points (b) Geometrical relationship of mark points

3.3 Experiment procedure

The drive motor together with the traction sheave is started with a preset constant acceleration and the load motor immediately outputs a constant loading torque during its start up. The constant inertial moment generated by the fly wheels due to the constant acceleration, together with the constant torque of load motor, are applied to the traction ropes as traction load. When the traction friction provided by this traction interface is lower than the total traction load, the rope slippage on the traction sheave occurs. The traction interface was monitored and the rope slippage was recorded with the camera during this process.

4 RESULTS AND DISCUSSION

4.1 Slip evolution in wrapping contact zone

Experiments were first conducted to investigate the slip evolution process in the wrapping contact zone, which was partitioned as head region, central region and end region. Note that the head region corresponds to the releasing part of the rope on the sheave. Camera measurement method was adopted to capture the rope slip behavior at the traction interface. In these experiments, about 130 pictures of marked regions in total were taken. However, only 6 pictures with equal time interval in each marked region were selected for slippage demonstration. The selected pictures in different regions are shown in Fig.5 and an obvious relative slip was observed between the marked points on the rope and the corresponding reference points on the sheave in both head and end regions as shown in Fig.5a and Fig.5c, especially in the last picture of each mark set. However, the relative slip is trivial and ignorable in mid region as shown in Fig.5b.

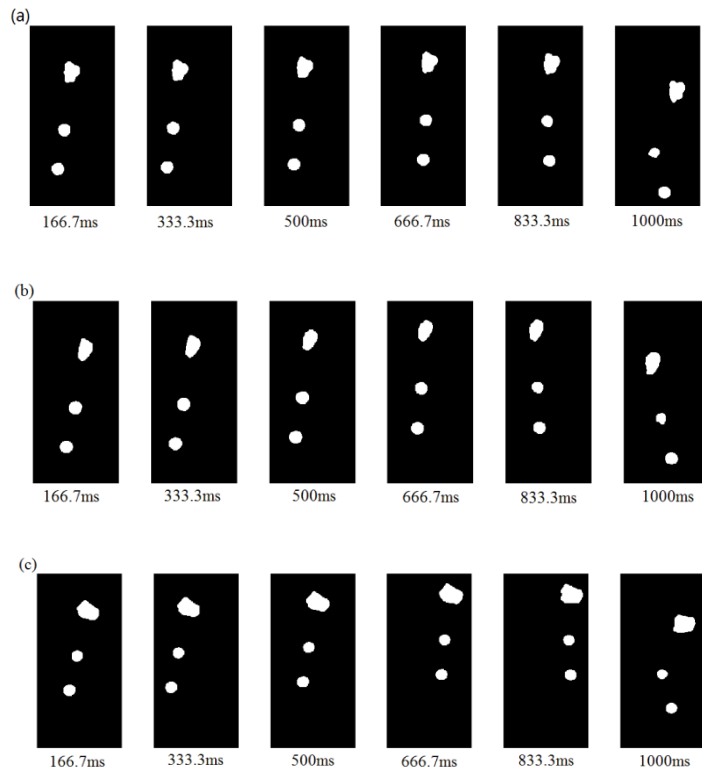


Figure 5 Image sequences of mark points in different regions: a. Head region; b. Mid region c. End region

Following the process in section 2.2, the slippage in different regions can be quantitatively obtained and the slippage developments in different regions are compared in Fig. 6. It can be observed that the slippage in both head and end regions increases sharply after it reaches the approximate critical value 800ms. However, the slippage development of mid region is extremely slow in the whole process. Based on the slippage data, it can be postulated that slipping occurs firstly at both ends of contact arc, and then expands to the middle region gradually until the full slip along the sheave occurs. Note that those marked points will be out of the shooting scope of the camera at about 1000ms, thus the fully slip in the whole contact region is not captured.

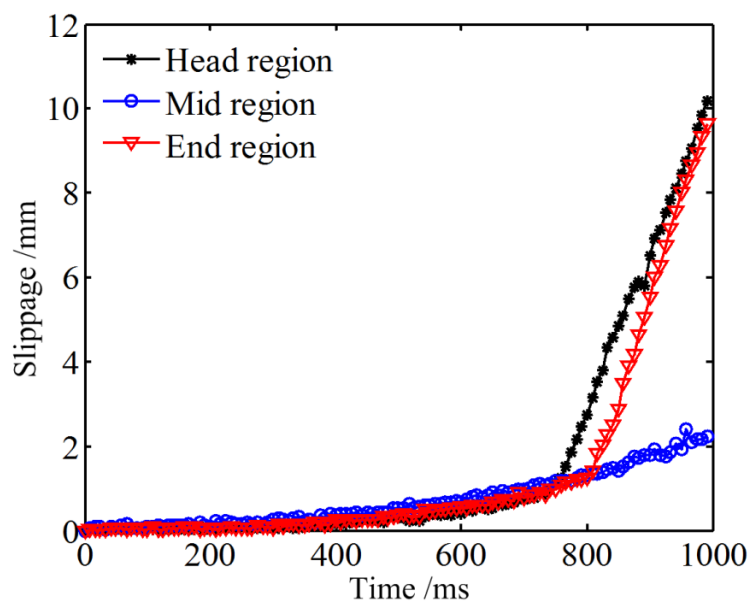


Figure 6 Experimental observation of slippage development in different regions

4.2 Effect of rope preload on slippage development

Two experimental tests, with a rope preload of 3500N and 1800N respectively, were carried out to investigate the effect of rope preload on the slippage development and the results are shown in Fig.7. Note that rope tension at both ends can be obtained by monitoring the corresponding reaction forces and the torque applied to the traction sheave by rope was induced by an imbalance of tension between these two ends of the rope. As shown in Fig.7, this imbalance keeps increasing until the friction force between the rope and sheave reaches the maximum value, after which, a full slip occurs and the rope-end force becomes approximately constant. It can also be observed from Fig.7 that with a lower rope preload, the full slip occurs earlier. Note that effect of pretension on equivalent COF can be also demonstrated by these tests. The rope-end force when slip is occurring can be experimentally measured and the wrap angle is known as 120° in the experiments, then according to Euler's equation, the equivalent COF values can be obtained as 0.405 for a preload of 1800N and 0.491 for a preload of 3500N respectively.

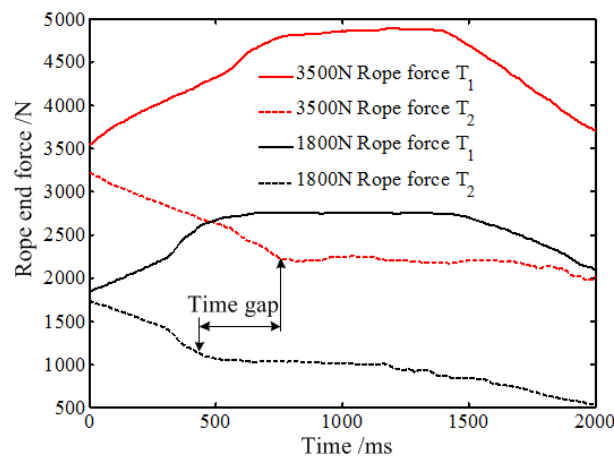


Figure 7 Instantaneous rope-end force behavior under two different pre-loads

The measured instantaneous slippage of head region under two preload levels are plotted in Fig.8. In both cases for head region, a sharp increase of slippage, which means a full slip, occurs at around $t=750$ ms and in low preload case rope slips a little bit earlier. It also can be observed that slippage for 1800N case increases more sharply than that for 3500N case once full slip initiates in these specific experimental tests.

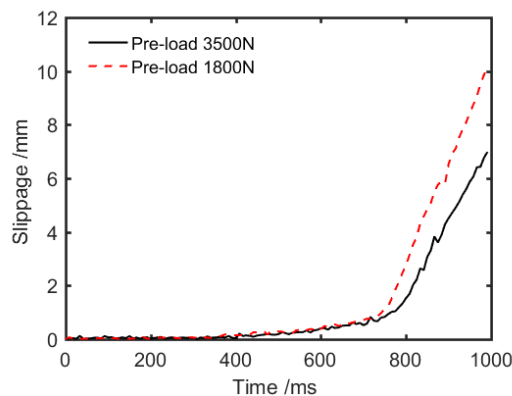


Figure 8 Slippage development of head region under different pre-tension forces

In order to double-check the effect of pre-load on the slippage, the instantaneous rotation speeds of drive motor and load motor were measured with encoders and the speed difference indicates the

slippage. The results are plotted in Fig.9a and Fig.9b, corresponding to a preload of 3500N and 1800N respectively. Obviously, a speed difference between drive motor and load motor appears at about $t=1050\text{ms}$ for 3500N case and $t=800\text{ms}$ for 1800N case, which double confirmed the previous conclusion that full slip occurs earlier under low preload condition. Note that the occurring time of slip measured by camera measurement method and by motor speed difference method are different because the time sequences between both measurement methods do not align.

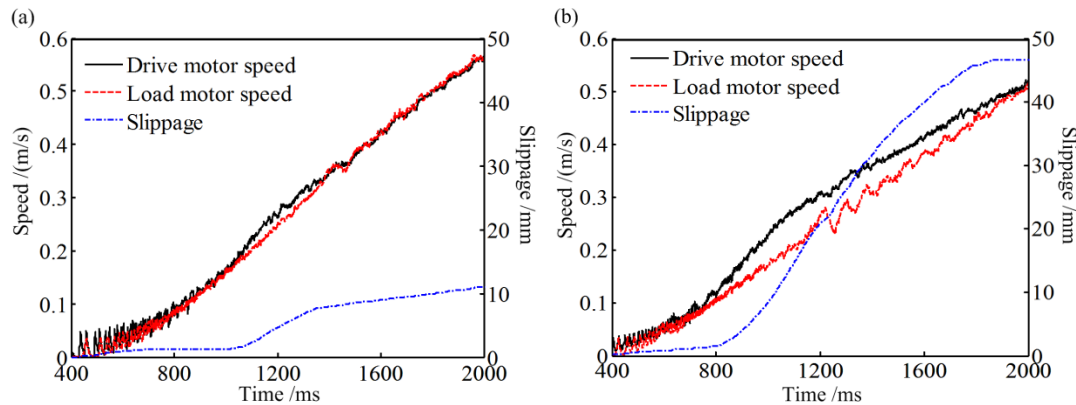


Figure 9 Instantaneous speeds of drive motor and loading motor with a preload of (a) 3500N (b) 1800N

5 CONCLUSIONS

In this paper, some experiments were performed to investigate slippage development at the traction interface between the rope and the sheave. Based upon these results, the following conclusions are obtained:

1. The camera measurement method for slippage monitoring proposed in this work is effective.
2. For the rope-traction sheave interaction model presented in this work, the slip occurs first at both ends, and then expands to the middle region gradually.
3. The full slip occurs earlier under lower pre-load.

6 LITERATURE REFERENCES

REFERENCES

- [1] Eytelwein, J.A., 1793, Ausgaben größtentheils aus der angewandten mathematik. Freidrich Manrer, Berlin, Germany.
- [2] Euler, M.L., 1762, Remarques sur l'effect du frottement dans l'équilibre. Mem. Acad. Sci., **18**:265-278.
- [3] Heller, S.R., 1970, The contact pressure between rope and sheave. Naval Engineers Journal, **82**(1): 49-57.
- [4] Usabiaga, H., Ezkurra, M., Madoz, M., and Pagalday, J., 2006, Mechanical interaction between wire rope and sheaves. Proceedings of the OIPEEC Conference "Trends for Ropes: design, application, operation," Athens, Greece.

- [5] Lugrís, U., Escalona, J.L., Dopico, D., and Cuadrado, J., 2011, Efficient and accurate simulation of the rope–sheave interaction in weight-lifting machines. *Proceedings of the Institution of Mechanical Engineers, Part K: Journal of Multi-body Dynamics*, **225(4)**: 331-343.
- [6] Nabijou, S., and Hobbs, R.E., 1995, Relative movements within wire ropes bent over sheaves. *The Journal of Strain Analysis for Engineering Design*, **30(2)**, 155-165.
- [7] Hobbs, R.E., and Nabijou, S., 1995, Changes in wire curvature as a wire rope is bent over a sheave. *The Journal of Strain Analysis for Engineering Design*, **30(4)**, 271-281.
- [8] Nabijou, S., and Hobbs, R.E., 1995, Frictional performance of wire and fibre ropes bent over sheaves. *The Journal of Strain Analysis for Engineering Design*, **30(1)**: 45-57.
- [9] Wiek, L., 1982, The distribution of the contact fores on steel wire ropes. *OIPEEC*, **44**, 10-25.
- [10] Usabiaga, H., Ezkurra, M., Madoz, M.A., and Pagalday, J.M., 2008, Experimental test for measuring the normal and tangential line contact pressure between wire rope and sheaves. *Experimental Techniques*, **32(5)**: 34-43.
- [11] Feyrer, K., 1986, Pressure between tape and pulley. *OIPEEC Bull*, **52**, 23-31.
- [12] Ridge, I.M., Zheng, J., and Chaplin, C.R., 2000, Measurement of cyclic bending strains in steel wire rope. *The Journal of Strain Analysis for Engineering Design*, **35(6)**, 545-558.
- [13] G.Z. Chen, Z.C. Zhu, Q. Lu, L.J. Zhou, G.H. Cao, Research on wireless detection policy of the friction lifting's sliding. *Proceedings of 2009 IEEE International Conference on Computational Intelligence for Measurement Systems and Applications (CIMSAS 2009)*, 2009, May 11–13. Hong Kong, China 2009, pp. 80–85.
- [14] Oplatka, G., and Roth, M., 1999, “Safety of Ropeway Drives Against Slipping Monitoring of Rope Slipping Using a Camera” .*International Organization for the Study of Transportation*, San

BIOGRAPHICAL DETAILS

Xiaolong Ma received the B.Sc. degree in mechanical engineering from Harbin Institute of Technology, China, in 2014. He is currently pursuing the Ph.D. degree at the School of Mechanical Engineering, Shanghai Jiao Tong University, China, under the supervision of Prof. Xi Shi. His research interests cover many aspects of dynamics and friction interface applied to elevator.

Prof. Xi Shi received his Ph.D. in Mechanical Engineering from University of Illinois at Urbana-Champaign in 2005. Currently, he is the director of Elevator Test Center at Shanghai Jiao Tong University. His research interests span from intelligent elevator technology and interfacial mechanics, to tribology. He has been the PI for tens of research projects sponsored by NSFC, MOST, MOE and international renowned enterprises, and published tens of journal papers. Prof. Xi Shi won the ASME K.L. Johnson Best Paper award in 2007.